Chem Soc Rev

Excitation energy migration dynamics in upconversion nanomaterials

Journal:	*Chemical Society Reviews*
Manuscript ID:	CS-TRV-05-2014-000168.R2
Article Type:	Tutorial Review
Date Submitted by the Author:	14-May-2014
Complete List of Authors:	Zhang, Hong; University of Amsterdam, Molecular Photonics - vant Hoff Institute for Molecular Sciences (HIMS) Langping, Tu; Chinese Academy of Sciences, Liu, Xiaomin; Changchun Institute of Optics, Fine Mechanics and Physics, Chinese Academy of Sciences, Key Laboratory of Excited State Processes Wu, Fei; Changchun Institute op Optics, Fine Mechanics and Physics, Chinese Academy of Sciences, State Key Laboratory of Luminescence and Applications

Excitation Energy Migration Dynamics in Upconversion Nanomaterials

Langping Tu[abc], Xiaomin Liu[ab], Fei Wu[abc], Hong Zhang[ab]*

a. State Key Laboratory of Luminescence and Applications, Changchun Institute of Optics, Fine Mechanics and Physics, Chinese Academy of Sciences, Changchun 130033, China.

b. van't Hoff Institute for Molecular Sciences, University of Amsterdam, Science Park 904, 1098 XH Amsterdam, The Netherlands.

c. Graduate University of the Chinese Academy of Sciences, Beijing 100049, China

Abstract:

Recent efforts and progresses in unraveling the fundamental mechanism of excitation energy migration dynamics in upconversion nanomaterials are covered in this review, including short- and long-term interaction and other interactions in homogeneous and heterogeneous nanostructures. Comprehension of the role of space confinement in excitation energy migration process is updated. Problems and challenges are also addressed.

*Corresponding author: h.zhang@uva.nl

1. Introduction

Upconversion luminescence, *i.e.* emission of one photon upon excitation of several lower energy photons, is very attractive for applications in broad fields. In recent years, the development of nanotechnology have been boosting the scientific interest, especially the interest of biomedical field, in relevant material systems, typically lanthanide ions doped nanomaterials. These nanomaterials, capable of converting the NIR photons to higher energy photons ranging from ultra violet (UV) to NIR, allow the excitation to fall in so-called "optical window" (~650-1300 nm), *i.e.* minimal absorption spectral range of human tissue and negligible autofluorescence of the biological background. They are thus expected to be able to improve significantly the quality of luminescence biomedical imaging, labelling and therapy. They are also regarded as potential candidates for improving solar energy utilization by converting NIR part of the solar spectrum to visible to match the absorption of commercially available solar cells. In these years, proof-of-concept reports continue to emerge. Despite these progresses, the unsatisfactory upconversion efficiency remains one of the main hurdles on its way to actual application. Although the excitation density of realizing observable upconversion in these materials is much lower than that of coherent sum-frequency generation, the upconversion efficiency is only several percent in a macroscopic crystal under 980 nm excitation, and the highest upconversion efficiency in nano-size materials so far is even more than one order of magnitude lower under the same excitation condition. For example, under 980 nm excitation of 150 Wcm^{-2} the highest upconversion quantum yield is reported around 0.1% for Yb^{3+}/Er^{3+} co-doped $NaYF_4$ core/shell nanoparticles of 30 nm in diameter.[1]

This situation has triggered following questions: What are the responsible channels/steps for the excitation energy loss in the nanomaterials? And more interestingly, is it possible to gain even higher upconversion efficiency in nanomaterials than in macroscopic crystals? In order to get answers of these questions, a comprehensive picture of how the excitation energy migrates in nanostructures is essential.

1.1. Fundamentals of upconversion dynamics

Three major upconversion mechanisms have been elucidated from the studies of macroscopic crystals, *i.e.* excited state absorption (ESA), energy transfer upconversion (ETU), and photon avalanche (PA). In all of these categories, ETU is the most popular one since it has high efficiency (about two orders of magnitude higher than ESA),[2] and is less susceptible to external conditions. When doped simply with one rare earth element as activators at low concentration, *i.e.* without sensitizing ions, interaction between the activators can be neglected. In this case ESA is responsible for the upconversion. With the increase of the doping concentration, interaction between the centers is becoming significant and the centers can no longer be simply treated as activators any more, instead they are also sensitizers, *i.e.* they will transfer the excited energy to other activators to assist the upconversion luminescence of the latter via ETU mechanism. It is also popular that sensitizer and activator are different dopants. So far, most of the commonly used upconversion schemes, such as Yb^{3+}/Er^{3+}, Yb^{3+}/Tm^{3+}, Yb^{3+}/Ho^{3+} co-doped combinations, are all recognized to follow the ETU mechanism.

From luminescence dynamics point of view, the upconversion process of rare earth ions doped systems can roughly be separated into three stages, including: excitation energy absorption, various energy transfer & upconversion and radiative release of the excitation energy, *i.e.* emitting upconversion photons. The popularly used parameter "luminescence quantum yield" characterizes only the efficiency of converting absorbed energy to emission in quanta. Excitation (absorption) efficiency, *i.e.* the efficiency of the first stage of the upconversion dynamic process, is not included. However, a robust upconversion spectrum relies not only on a high upconversion emission quantum yield, but also on a large absorption cross section. This is the starting point of developing approaches in improving upconversion emission.

1.2. Characteristics of upconversion luminescence in nanosystems

Compared with macroscopic crystals, materials of nanometer size exhibit three

distinct properties which are important for the upconversion emission. The first distinct property would be the nonnegligible role of the surface properties which is due to the relatively large surface-to-volume ratio of nanomaterials. It should be notice that although surface can form energy traps which usually quench the upconversion luminescence, it can be beneficial as well. For example, enhancement and/or broadening of absorption can be realized by anchoring organic molecules or other light harvesting entities onto the surface of upconversion nanoparticles. In addition, the high-frequency vibration modes of surfactants and/or other organic entities on the surface are widely acknowledged to assist the population relaxation between two electronic states of the activators/sensitizers inside the nanoparticles,[3,4] although the interaction mechanism remains vague.

The second distinct property is that nanomaterials allow tailor-made internal structure. More and more complex nanostructures are becoming possible due to the development of nanotechnology. This property has raised aspiration that the excitation energy might be "fully conserved" for upconversion emission since, if a tiny defect-free crystalline domain in a nanoparticle can be "isolated" from its neighbors (which might contain defects), the absorbed energy in this area in theory can be free of nonradiative loss. Concentration quenching effect, *i.e.* the excitation energy is easier to migrate from one ion to another under high doping concentration, which increases the probability for the energy to be trapped by the defects inside and/or at the surface of the nanoparticles, could thus be suppressed. Therefore, higher upconversion efficiency could be expected in specially designed nanostructures. This property brings in also opportunities to revisit conventional upconversion mechanisms. In conventional macroscopic crystals sensitizers and activators could not be separately located in the crystal. Hence the contribution of energy transfer between sensitizers has hardly been studied. In specially designed nanomaterials, however, it is becoming readily detectable. For example, in core/active shell nanoparticles where sensitizers are also doped in the shell the excitation energy absorbed in the shell can contribute to upconversion emission after a long trek to reach the activators inside the core, although the exact role it plays needs to be further elucidated.

Excitation energy migration in a typical rare earth ions doped core/shell nanoparticle is depicted in Fig. 1, where the involved interactions include, among others, forward- and backward energy transfer between a sensitizer and an activator, the energy transfer among sensitizers, cross relaxation between activators, the interaction between activators/sensitizers and surface related entities, *e.g.* high-frequency vibrational modes of organic entities and other surface quenching centers. Spectroscopy, in combination with structural modulation and doping variation in elements and concentrations in a nanosystem, is a powerful tool in unravelling these interactions. For example, doping only sensitizing ions allows us to acquire the energy transfer information between the sensitizers by monitoring the sensitizer luminescence and relevant temporal behavior. Furthermore, if activators are co-doped in, the luminescence decay of the sensitizer shall speed up and the energy transfer mechanism between the sensitizer and the activator can thus be elucidated. Cross relaxation can be monitored by, *e.g.*, populating different electronic states. Effect of the surface related entities can be clarified by the dependence of the upconversion spectrum on the interaction distance, *e.g.* the shell thickness or the length of the organic chain between the luminescence activators/sensitizers and the entities.

The third distinct property of nanomaterials is that it is susceptible to the environment due to the size limit. Compared with the macroscopic crystals, the nanomaterials are more susceptible to the environment, which makes external stimuli more effective in modifying upconversion dynamics by, *e.g.* modifying the transition moments involved in the upconversion. Let's look at a simple interaction picture between light and matter. Considering a two level emission center, the emission and absorption probabilities are proportional to the square of the transition moment between the two levels and the population of the initial level. The transition moment is subject to the local electric field. For rare earth ions doped nanosystems, the transition moments could be varied if the local crystal field of the nanohost is changed due, for example, to externally applied electric field. This provides another possibility to improve the efficiency of upconversion emission, *i.e.* applying external electric field to enhance the absorption and/or upconversion emission, and/or modulating the

transitions in the intermediate energy transfer processes.

In recent years more and more attention has been paid on the upconversion mechanism in nanosystems aiming at high upconversion efficiency and controlled spectral modulation. Here we shall review these efforts and relevant progresses achieved so far, update our comprehension of upconversion dynamics in nanosystems and present our perspectives of the research in the coming period. The review is organized along the axis of effects of excitation on upconversion emission, energy transfer & interaction and transition probability enhancement.

2. Effect of excitation on upconversion emission

The upconversion emission starts with the light absorption. Different excitation approaches will lead to the variation of upconversion dynamics, resulting in different upconversion spectra and upconversion efficiencies. Various excitation patterns have been proposed in the past years aiming at the elevation of upconversion efficiency, and/or at spectral modulation, and/or at potential applications. In order to have robust upconversion luminescence, excitation must be efficient. The excitation rate R of state i can be described as:

$$R_{\mathrm{i}} \propto I_{exc}\sigma_{\mathrm{i}}N_{\mathrm{i}} \qquad (1)$$

where σ_{i} is the absorption cross section of the state i at the excitation wavelength and N_{i} is its population density, I_{exc} is the excitation density. From this relation it is obvious that absorption cross section is key in determining the excitation efficiency. In this section we shall review efforts and progresses in improving excitation efficiency of upconversion nanomaterials, mainly covering different excitation wavelengths approach, co-doping approach, broadband excitation approach.

2.1. Singly doped upconversion

Lanthanides are a group of elements in the periodic table where the 4f inner shell is (partially) filled with electrons. They are mostly stable in the trivalent form (Ln^{3+}) and the Ln^{3+} ions have the electronic configuration $4f^n\,5s^2\,5p^6$ where n varies from 0 to

14. The 4f electrons are shielded by the completed filled $5s^2$ and $5p^6$ orbitals resulting in weak electron-phonon coupling and the f-f transitions are in principle parity forbidden. Consequently, their absorption and emission are featured by narrow f-f transition bands with low transition probabilities and substantially long lifetimes. Therefore one electron in excited state may have a high chance to reach a higher excited state by absorbing a second photon (ESA) or resonating with another excited electron (ETU). Theoretically, the upconversion emission can be expected in most singly doped lanthanide ions.[2] With the increase of doping concentration, ETU, instead of ESA, is becoming dominant in upconversion. The ETU process has high requirements for energy level matching. Since strictly well-matched ladder-like energy levels are not usually obtainable, the process often asks for phonon assistance. From this point of view, proper choices of host material and measurement temperature are crucial for upconversion emission. However, the effort of increasing doping concentration is restricted by concentration quenching effect. Er^{3+} is special in this aspect. Singly doped Er^{3+} ion has comparatively high upconversion efficiency since its optimal doping concentration can reach a relatively high level and its ladder-like energy levels are well matched with ~800, ~980 and ~1500 nm excitation, respectively, as is shown in Fig. 2. Under ~1500 nm laser excitation, the upconversion luminescence quantum yield is high up to $\sim 1.2 \pm 0.1\%$ under excitation density of 1.5×10^6 W/m^2 in nano-sized $LiYF_4$ host[5] and $\sim 12 \pm 1\%$ under excitation power density of 700 W/m^2 in micron-sized Gd_2O_2S host.[6] Such high quantum yields contain both the visible and NIR emission contributions. Considering that the terrestrial AM1.5 solar spectrum possesses 25 W/m^2 of energy in the range of 1480-1580 nm and the upconversion emissions fall in the c-Si absorption range, Er^{3+} has potential application in solar spectrum conversion. According to Rodríguez *et al.* the ETU process dominants the conversion between IR photons (1500 nm) to NIR photons (980 nm) under 1500 nm excitation, meanwhile, both ETU and ESA contribute to the green upconversion emission from the $^4S_{3/2}$ level.[6]

2.2. Yb^{3+}- sensitized upconversion

As noted before, most lanthanide activator ions in singly doped nanocrystals demonstrate inferior absorption. In addition, the concentration of activator ions has to be maintained at low level and precisely adjusted to avoid significant concentration quenching. Therefore the overall upconversion efficiency of most singly doped nanocrystals is relatively low. To enhance the upconversion luminescence efficiency, a popular approach for macroscopic crystals is adopted for nanosystems where a sensitizer with a reasonable absorption cross-section in the NIR region is co-doped along with the activator when an efficient ETU process exists between the two. Trivalent Yb^{3+} possesses an extremely simple energy level scheme with only one excited 4f level of $^2F_{5/2}$ in the interesting range. The absorption band of Yb^{3+} is due to the $^2F_{7/2}\rightarrow{}^2F_{5/2}$ transition, which is located around 980 nm and has a relatively large absorption cross-section (1.2×10^{-20} cm^2) compared with that of Er^{3+} ions (1.7×10^{-21} cm^2). Additionally, the $^2F_{7/2}\rightarrow{}^2F_{5/2}$ transition of Yb^{3+} is well resonant with the typical upconverting lanthanide ions, such as Er^{3+}, Tm^{3+}, and Ho^{3+}, thus can significantly improve the upconversion efficiency. Yb^{3+} has also been used to sensitize some transition metals (TMs) for upconversion emission, such as Ni^{2+}, Mn^{2+}, Cr^{3+}, and Re^{4+}.[7] Since the upconversion emission of the transition metal ions depends strongly on the crystal field, the emission can be tailored for particular solar cell applications via suitable chemical variations of the host lattice.

Usually Yb^{3+} is co-doped into the crystal lattice with a proper concentration (20~40%). Higher doping concentration of Yb^{3+} can improve the absorption, but, in the meantime, leads to the cascade energy transfer process more probable in a nanoparticle and the concentration quenching effect becomes severe. However, there are some specially designed structures where the quenching concentration of Yb^{3+} is improved as the consequence of adjusted energy transfer process, which will be introduced in section 3.2.2. Another approach to increase the amount of Yb^{3+} ions is to make use of the space feature of the nanoparticles. For example, shell coating is a commonly used strategy to enhance the upconversion emission of a nanoparticle by separating the surface relevant quenching centers and the luminescence centers inside the core. In the majority of the reported cases, the shell is inert, *i.e.* a shell of pure host

lattice, and its sole role is to protect the luminescence centers in the core from the surface. Since 2009, new design of the core/shell structure appears which contains sensitizer Yb^{3+} in the shell *i.e.* "active shell". The first report by Vetrone *et al*. was on $NaGdF_4$: Yb^{3+}, Er^{3+} nanoparticles with a shell containing 20% Yb^{3+}-doped $NaGdF_4$ where strong enhancement of the green and red emission bands was realized.[8] Additional energy transfer from excited Yb^{3+} ions in the shell to the Er^{3+} ions in the core was suggested to be responsible for the increase of the overall upconversion efficiency of the particles. The upconversion emission of the active core-active shell nanoparticles is about three times (for the green emission) and ten times (for the red emission) stronger than that of the active core-inert shell counter parts. Further studies of other groups indicate that the emission enhancement induced by an active shell comes solely from the increase of the absorption efficiency. It should be noted, however, that the sensitizers in the shell are close to the surface which is harmful for upconversion emission since it increases the probability of the excitation energy being captured by the surface related traps. Obviously, the actual role of active shell in upconversion dynamics is unclear yet. Systematically study and revisit of these results are demanding.

2.3. Nd^{3+} and Yb^{3+} cooperative sensitization

The Yb^{3+}-sensitized upconversion nanoparticles (UCNPs), regarded as a new generation of multimodal bio-probes, have been attracting wide interest in biological applications. But the single narrow band absorption nature of the Yb^{3+}-sensitized upconversion process obstructs the relevant *in vivo* applications. Excitation around 980 nm can still be absorbed by water - the most significant component of animal and human body and causes local heating. In the context of *in vivo* applications, the overheating is an undesirable side-effect that can reduce cell viability and induce tissue damage especially when long-duration laser exposure or relatively high excitation power density is needed. Various attempts have been reported to set the excitation wavelength away from this spectral region. One of them is using a CW laser excitation at 915 nm, instead of 980 nm, to reduce the radiation heating to a

certain extent at the expense of upconversion efficiency.[9] Another approach is to introduce Nd^{3+} ions as an additional NIR absorber and sensitizer in the conventional Yb^{3+}-doped UCNPs. The $Nd^{3+}\rightarrow Yb^{3+}$energy transfer has high efficiency and this effective energy transfer is expected to extend the excitation spectral range of the conventional Yb^{3+}-doped UCNPs from the narrow band characteristic of Yb^{3+}, because Nd^{3+} has multiple NIR excitation bands shorter than 980 nm, such as 730, 808, and 865 nm, corresponding to transitions from $^4I_{9/2}$ to $^4F_{7/2}$, $^4F_{5/2}$, and $^4F_{3/2}$, respectively. Importantly, water has negligible absorption at these wavelengths. Consequently, the laser-induced heating effect in biological tissues is expected to be greatly reduced. At the same time, Nd^{3+} has an even larger absorption cross-section in the NIR region (1.2×10^{-19} cm^2 at 808 nm) compared to Yb^{3+} (1.2×10^{-20} cm^2 at 980 nm),[10] which also benefits the efficiency of the Nd^{3+}-sensitized upconversion process.

Here are some typical examples of Nd^{3+} and Yb^{3+} cooperatively sensitized UCNPs. The first generation of the 808nm excitable Nd^{3+} sensitized UCNPs is a $Nd^{3+}/Yb^{3+}/Er^{3+}$ (Tm^{3+}) triply doped nanoparticles. Nd^{3+} ions take the role of absorbing photons around 800 nm, while the Yb^{3+} ions act as bridging ions for the energy transfer from the Nd^{3+} ion to the activator Er^{3+} (Tm^{3+}).[11] However, this cooperative sensitization design has several drawbacks. Firstly, Nd^{3+}can only be doped at very low concentration (typically ≤1%), the resulting weak absorption around 800 nm does not help very much to a robust upconversion emission. Secondly, the introduction of Nd^{3+} as sensitizer may directly quench the upconversion emission, owing to the deleterious energy back-transfer from the activators to Nd^{3+}. Improvement is realized by spatially separating the two sensitizers, *i.e.* $NaGdF_4$: Yb^{3+}, Er^{3+} @ $NaGdF_4$: Nd^{3+}, Yb^{3+} UCNPs.[10] In this smart design by Wang *et al.* the core is doped with Yb^{3+} and activator Er^{3+}, where the Yb^{3+} sensitized UC process is supposed to occur, and the shell is doped with Nd^{3+} and Yb^{3+}, where the excitation of Nd^{3+} and subsequent $Nd^{3+}\rightarrow Yb^{3+}$ energy transfer could take place (Fig. 3). Under 808 nm excitation this structure enhances upconversion emission by ~7 times compared with the triply doped UCNPs without spatial separation. Xie *et al.* reported the $NaYF_4$: Yb^{3+}, Tm^{3+}, Nd^{3+} @ $NaYF_4$: Nd^{3+} structure with relatively high concentration of Nd^{3+} (~20 mol%)

in the shell layer and thus enhanced markedly the upconversion emission.[12] The key in this design is to increase the doping concentration of sensitizer Nd^{3+} ions to such that quenching interaction between the Nd^{3+} ions and activators will not occur. Lately, Zhong *et al*. have introduced a transition layer into the sensitizer Nd^{3+} and activator Er^{3+} spatially separated core-shell structure $NaYF_4$: Yb^{3+}, Er^{3+} @ $NaYF_4$: Yb^{3+} @ $NaNdF_4$: Yb^{3+}.[13] This unique nanostructure is essential to eliminate the deleterious cross relaxation pathways between the activator and sensitizer by means of a precisely controlled transition layer. Upon 800 nm excitation the upconversion emission reaches maximum when the interlayer thickness is about 1.45 nm.

2.4. Broad-band sensitization

From the viewpoint of solar energy utilization, it is of great interest for an efficient conversion of NIR part of the solar spectrum, which is wasted in most applications, to visible region. The commonly used NIR sensitizers, *e.g.* Yb^{3+} or Nd^{3+}-Yb^{3+} pair, are not ideal in this aspect because of the narrow f-f absorption bands. Assistance of other materials to extend NIR absorption thus becomes an option. A proper sensitizer must match several criteria: Firstly, it must have a broad absorption spectrum with sufficient cross-section in the NIR region. Secondly, it must have emission that overlaps in spectrum with the absorption of the upconverting ions, and thirdly, the sensitizer should not absorb in the visible region and especially not at the wavelengths where the upconversion luminescence is expected, and finally it should be photostable.

2.4.1. Transition metal ion sensitization

The ligand field dependence of the exited states of the transition metal (TM) ions could be used for tuning the energy levels of the sensitizing ion to match the required acceptor or chemically varying the host lattice. In addition, co-doping Ln^{3+}/TM into the same host lattice could lead to new types of cooperative upconversion mechanisms. A variety of ion couples have been imported to demonstrate this upconversion scheme. An insightful review was provided by Suyver *et al.* concerning

NIR broad-band sensitizers for upconversion where the transition metal ions are directly involved in the upconversion process.[14]

2.4.2. Infrared organic dye sensitization

In addition to the transition metal ions, infrared organic dyes have been selected as antenna ligands to enlarge the absorption spectrum for upconversion. Recently, Zou *et al.* reported the sensitization of β-$NaYF_4$:Yb^{3+}, Er^{3+} nanoparticles by organic infrared dye (IR-806).[15] The extinction coefficient of IR-806 at 806 nm is 390 $l \cdot g^{-1} \cdot cm^{-1}$, which is ~$5 \times 10^6$ times higher than that of β-$NaYF_4$:Yb^{3+}, Er^{3+} nanoparticles at 975 nm (7×10^{-5} $l \cdot g^{-1} \cdot cm^{-1}$). The overall upconversion emission of the dye-sensitized nanoparticles is dramatically enhanced (by a factor of ~3,300) as a joint effect of the increase and overall broadening of the absorption spectrum. The monochromatic quantum yield of the IR-806-nanoparticle complex was determined to be $0.12 \pm 0.05\%$ under 800 nm excitation at the intensity saturation point for monochromatic illumination, whereas the quantum yield of non-sensitized nanoparticles was only $0.3 \pm 0.1\%$ under excitation at the maximum absorption wavelength of 975 nm. However, in our opinion further confirmation of the huge improvement is necessary. By using suitable co-sensitizing sets of antenna molecules and proper upconverting nanoparticles, broader NIR part of solar spectrum is expected to be absorbed for upconversion with higher efficiency. Nevertheless, most organic molecules suffer from photobleaching, which brings the concern on the photostability of the organic dye sensitized nanomaterials.

3. Energy transfer & interaction

Energy transfer and interaction are critical for the upconversion emission. Recently, efforts have been put to elucidate the speciality of these processes in the space confined systems and the impact on the upconversion processes, which has brought possibilities to improve the upconversion efficiency and/or to tune the excitation/emission spectra. In the meantime, some puzzles remain to be disentangled.

3.1.The mechanism of ETU

3.1.1. The basic model – short range ETU interaction

The basic model of ETU process was established several decades ago. As a conceptual picture, a simplest upconversion system with two-level donors and three-level acceptors is used here, as shown in Fig. 4. The ETU process can be described by the following equations:

$$\begin{aligned}\frac{\mathrm{d}n_{D1}}{\mathrm{dt}} &= \rho_{exc}\sigma n_{D0} - W_0 n_{D1} n_{A0} - W_1 n_{D1} n_{A1} - A_{D1} n_{D1} \\ \frac{\mathrm{d}n_{A1}}{\mathrm{dt}} &= W_0 n_{D1} n_{A0} - W_1 n_{D1} n_{A1} - A_{A1} n_{A1} \\ \frac{\mathrm{d}n_{A2}}{\mathrm{dt}} &= W_1 n_{D1} n_{A1} - A_{A2} n_{A2}\end{aligned} \quad (2)$$

where $n_{D0,1}$, $n_{A0,1,2}$ are the populations of each energy levels of the donor and acceptor, respectively ρ_{exc} is the laser photon number density, σ is the absorption cross section of the donor ion, W_1, W_2 are the energy transfer coefficients from n_{D1} level to n_{A0}, n_{A1} levels, respectively, A_{D1}, $A_{A1,2}$ are the decay rates of the corresponding energy levels. The details of this model have already been intensively discussed.[2,16] However, it is worth noting that in this model, the difference caused by spatial distribution of the donor and accepter might be overlooked since the energy transfer coefficients (W_0 and W_1) take the statistically average values. Here the ETU process can be simplified to an energy transfer process between two neighboring donor-acceptor ions, which we named as "short-range energy transfer model" in this text. Although the energy migration between donors before it is transferred to an acceptor was proposed in some initial papers,[17] in most actual instances, high donor concentration often leads to assumption that the energy migration process is very fast.[2,17] This "fast migration" approximation has been widely accepted in upconversion studies of the donor and acceptor co-doped systems. The role of the migration process in upconversion mechanism was often ignored until recently.

3.1.2. The energy migration upconversion (EMU)– long range ETU interaction

In recent years, to meet the requirements of special applications and accompanied

with the progress in synthetic technology of nanomaterials, more complex upconversion nanostructures have been reported, in which some have donor and acceptor partially or completely separated in space and bright upconversion emission was surprisingly observed. The ETU process in these structures was described as follows: the energy of excited states randomly hops step-by-step between donors, before trapped by the acceptor ions for upconversion emission. Different from the basic ETU model, it is a relatively "long-range" interaction process which was named by Wang *et al.* as "energy migration-mediated upconversion" (EMU) process. In 2011, they designed a donor and acceptor spatially separated core-shell-shell structure,[18] as shown in Fig. 5. The excitation energy is accumulated in the core area by a Yb^{3+}-Tm^{3+} upconversion process, followed by energy transfer from Tm^{3+} ($^1I_6$) to Gd^{3+} ($^6P_{7/2}$). The energy then randomly hops between Gd^{3+} ions in the middle layer and finally captured by the acceptor ions (Eu^{3+}/Tb^{3+}/Sm^{3+}/Dy^{3+}) doped in the outer layer for upconversion emission. In this structure, in order to have an efficient upconversion emission, the harvested UV energy should be able to travel quite a long distance (can be longer than 5 nm) without significant loss through a Gd^{3+} sublattice in the $NaGdF_4$ host. Furthermore, it is interesting to note that besides the Gd^{3+} ions, some other rare earth ions (*e.g.* Yb^{3+}) have similar property. The "long-range" energy transfer of Yb^{3+} was supported by the strong upconversion emission of core/active shell structures,[10,12,13] especially by the Nd^{3+}-sensitized $NaYF_4$: Yb^{3+}, Er^{3+} @ $NaYF_4$: Yb^{3+} @ $NaYF_4$: Yb^{3+}, Nd^{3+} core-shell-shell structure designed by Zhong *et al.*, as shown in Fig.6.[13] Under 800 nm excitation the donor ions (Nd^{3+}) are excited in the outer layer. Since the acceptor ions (Er^{3+}) are located in the core area, the energy transfer from Nd^{3+} to Er^{3+} must be with the help of the Yb^{3+} ions in the interlayer through efficient energy migration between Yb^{3+} ions. Similar EMU process was also reported by Wen *et al.* in the $NaYbF_4$: Nd^{3+}@ $Na(Yb^{3+},Gd^{3+})F_4$: Er^{3+}@ $NaGdF_4$ core-shell-shell structure.[19] The efficient "long-range" EMU process implies that the energy transfer process is actually not a local effect. The energy could be captured by an acceptor far away from the donor (several nanometers) with the assistance of the mediate ions (such as Yb^{3+} and Gd^{3+}). Based on this comprehension, the EMU process may also play a role in

upconversion emission even in the donor-acceptor co-doping systems, which remains a subject to be further studied. From our point of view, priority could be given to "spatial separation structure" to study the EMU process. This specially designed structure allows the separation of absorption, transition and emission regions in different areas of a nanoparticle. By monitoring the emission spectrum of nanoparticles with different thickness of transition layer and doping concentration of the bridging ions in the transition layer, energy migration process in the transition layer could be well followed.

Besides steady state spectroscopy, the time-resolved spectroscopy is another powerful and convenient method in studying excited state dynamics. Temporal behavior of upconversion luminescence is often used to characterize upconversion dynamics. For example, in a recent report of Lu *et al.*[20] the lifetime of blue upconversion emission of activator (Tm^{3+}) shortens significantly from hundreds of microseconds to tens of microseconds when its concentration increases from 0.2% to 8%, under the presence of the sensitizer Yb^{3+} (20%). Similar result has also been reported in Yb^{3+}/Er^{3+} co-doping nanosystem.[3] These phenomena were usually ascribed to the interactions between activators (such as concentration quenching effect and/or cross relaxation interaction). This assignment deserves, however, a revisit because some fundamental relations have not yet been well established. For example, the possible role of EMU. On the other hand, it is well known that it is not always true that the rise of an emission corresponds to the emissive state population and the decay to the corresponding depopulation. Therefore it is risky to relate blindly the temporal behavior of the upconversion luminescence to specific upconversion processes without analyzing the dynamic processes in detail.

3.2. Important factors for ETU process

Generally speaking, the ETU process not only includes the energy transfer between the ions, but is also subject to the initial distribution of the excited states and the boundary conditions of the nanoparticles, *e.g.* surface property, size and morphology of the nanoparticles. The full description of the ETU process is therefore complex. In

this section we will introduce the main factors that affect the ETU process, including the donor-acceptor combination, doping concentration, the excitation power density and the surface effect.

3.2.1.Donor-acceptor combination

Because Yb^{3+} ion has a simple energy scheme and a relatively large excitation cross-section in the NIR region, it was considered as a good sensitizer to enhance the upconversion emission by Auzel in 1960s.[21] During the past decades, the most widely used donor-acceptor combination is Yb^{3+} co-doped with activators such as Er^{3+}, Tm^{3+} or Ho^{3+}. Recently, it was reported that introducing some new donor-acceptor combinations can manipulate the ETU process, and consequently change the excitation and/or emission spectra. As mentioned before, adding Nd^{3+} and availing oneself of the energy transfer between Nd^{3+} and Yb^{3+} can shift the excitation of the upconversion emission to ~800 nm. The obvious advantage of this design is the minimization of the overheating effect in biological systems induced by water absorption. On top of that, the upconversion emission spectrum can also be modulated by the doping elements. Single-band upconversion emission with high chromatic purity is known to be highly desirable for multicolor imaging applications, and efforts in this aspect appear recently in literature based on novel donor-acceptor combinations.[22-24] For example, the Er^{3+}/Tm^{3+} (2/2%) co-doped nanoparticles show a spectrally pure red emission due to the energy transfer between $Er^{3+}$and Tm^{3+} (as shown in Fig. 7a).[24] However, because of the insufficient absorption of Er^{3+}, the upconversion emission is relatively weak. Alternatively, Tian *et al.* and Wang *et al.* reported independently that additional doping of Mn^{2+} ions can bring in single-band emission in Yb^{3+}/Er^{3+}, Yb^{3+}/Tm^{3+}, Yb^{3+}/Ho^{3+} upconversion systems.[22,23] Taking Yb^{3+}/Er^{3+} as an example (Fig. 7b), the existence of Mn^{2+} ions was considered to disturb the transition possibilities between the green and red emissions of Er^{3+}, the Er^{3+}-Mn^{2+} energy transfer leads to depopulation of the green emitting $^2H_{11/2}$ and $^4S_{3/2}$ energy levels, and the consequent Mn^{2+}-Er^{3+} back energy transfer increases the population of red emitting energy level ($^4F_{9/2}$), resulting in an enhanced red to green

emission ratio of Er^{3+}. Besides, doping Ce^{3+} in the Yb^{3+}/Ho^{3+} system could increase the red to green emission ratio by tuning the energy transfer process between Ce^{3+} and Ho^{3+},[25] and the deep-ultraviolet upconversion emission of Gd^{3+} ions could be enhanced by doping Ho^{3+}, serving as a "bridging ion" in the Yb^{3+}-Ho^{3+}-Gd^{3+} energy transfer process.[26]

3.2.2. Doping concentration

The ETU process involves mutual interactions of the ions, which are usually considered as dipole-dipole or dipole-quadrupole interaction and are therefore sensitive to the operating distance. Doping concentration thus affects significantly the energy transfer process and the optical properties of UCNPs because it determines the distance between the dopant ions as well as the amount of the dopant ions in a nanoparticle.

As noted before, increasing the doping concentration of Ln^{3+} ions (either sensitizer or activator) in the nanoparticles could enhance the upconversion emission to certain extent. Further increase could make the cascade energy transfer process effective and concentration quenching phenomenon significant, as described in the introduction. Therefore, the optimal doping concentration of Ln^{3+} ions is usually at a relatively low level, *i.e.* in the range of 0.2~2% for activators (*e.g.* Er^{3+}, Tm^{3+} or Ho^{3+}) with 20~40% for sensitizer (Yb^{3+}). Over the years, great efforts have been paid to elevate the quenching concentration of Ln^{3+} ions in nanoparticles. Chen *et al.* reported in the ultrasmall (7~10 nm) $NaYF_4$: x% Yb^{3+}, 2% Tm^{3+} nanoparticles the Yb^{3+} ions can be doped with concentration as high as 98% before obvious quenching occurs.[27] The NIR upconversion emission of Tm^{3+} at 808 nm was demonstrated to increase up to 43 times along with an increase in the relative content of Yb^{3+} ions from 20% to 98%, which was ascribed to the electronic characteristic of the sensitizer Yb^{3+} being different from activator such as Er^{3+}, Tm^{3+} or Ho^{3+}. As introduced before, the energy scheme of Yb^{3+} is relatively simple and there is only one excited state $^2F_{5/2}$ in the energy range of our interest. The harmful cross relaxation process could therefore be excluded, thus the "concentration quenching effect" is suppressed.[28] However, this

particularly high quenching concentration of Yb^{3+} is only reported for activator Tm^{3+} co-doped case and there is no report of similar result for other activators like Er^{3+} or Ho^{3+}. This fact might indicate that the relevant quenching mechanism needs to be further elucidated. On the other hand, Liu *et al.* established a "dopant ions spatial separation" structure to enhance the quenching concentration of Er^{3+}.[29] As shown in Fig. 8, in the controlled fine multi-layer sandwich-like architecture, Er^{3+} ions are doped into separated areas of the nanoparticle and energy transfer between Er^{3+} ions in different areas is thus suppressed which enhances the quenching concentration of Er^{3+} from 2% to 5% in the 20% Yb^{3+} doped $NaYF_4$ host. Similar result was also reported in Nd^{3+}-sensitized upconversion structure. When Nd^{3+} ions are co-doped with activators (Er^{3+}, Ho^{3+}, Tm^{3+}) in the core area, the optimal doping concentration of Nd^{3+} is ~1%,[12] whereas a donor-acceptor spatially separated core-shell-shell structure elevates the optimal doping concentration to 90%.[13]

Another approach to shorten the energy transfer operating distance is to select proper hosts. Besides the popular $NaYF_4$, several other host materials have also been explored. For example, Na_xScF_{3+x} is found to be a host benefiting the red upconversion emission (660 nm) of Er^{3+}, which is ascribed to the small radius of Sc^{3+}. When Yb^{3+} replaces Sc^{3+}, the distance between Er^{3+} and Yb^{3+} cation pairs is shorter than that in $NaYF_4$ host.[30] Typically, Wang *et al.* used KYb_2F_7 host material to construct a more thorough "dopant ions spatial separation" structure at the sub-lattice level.[31] The specificity of the KYb_2F_7 crystal structure is that the Yb^{3+} ions are separated as arrays of discrete clusters at the sub-lattice level and the averaged distance between the ionic clusters is much larger than the ionic distance within the clusters, as shown in Fig.9. In this structure, the excitation energy absorbed by Yb^{3+} ions "tends" to be restricted within the cluster rather than migrates a long distance towards other clusters. In this way the concentration quenching effect can be suppressed significantly if these clusters are quenching-center free. Indeed the doping concentration of Yb^{3+} was elevated to 98% before obvious quenching. High sensitizer concentration and excitation energy confined in sensitizer-located favor also the upconversion of more photons, exampled by the symbolic increase of violet

upconversion emission of Er^{3+} ions.

Doping concentration is in direct relation with both the amplitude and the pattern of the upconversion emission spectrum. In some cases, it is found that concentration variation of sensitizers or activators could come to the same modification of the upconversion spectrum, but following different mechanisms. Higher sensitizer density might promote not only the absorption of the excitation energy, but also the energy migration among the sensitizers and probably also the back energy transfer (from activator to sensitizer), whereas the high activator density might elevate the probability of cross relaxation. For example, increasing the doping concentration of either Yb^{3+}or Er^{3+} in the Yb^{3+}/Er^{3+} co-doped nanoparticles could come to the same increase of red-to-green emission ratio. The increase of the amount of Yb^{3+} was argued to facilitate the back energy transfer from Er^{3+} to Yb^{3+}, and the increase of Er^{3+} was thought to aggravate the cross relaxation between Er^{3+} ions.[3] There are also reports on fine-tuning the output color through the doping concentration adjustment of Ln^{3+} ions, which is particularly interesting for multiplexed labeling.[32]

3.2.3. Excitation density effect

Upconversion emission is a non-linear process. In the year 2000, Pollnau *et al.* modeled the relationship of excitation density P with upconversion emission intensity I, which is $I \propto P^n$ under low excitation power density.[16] The value of n indicates the number of NIR excitation photons required to generate one upconversion photon. This popular and distinct description is based on a simplified upconversion picture and low density excitation assumption. Real energy migration/transfer occurring in a nanosystem could be more complex. Let's take Er^{3+} as an example. Under the excitation of 980 nm, both the 545 nm and 650 nm emission require two-photon process considering the energy match. However, the complex of the energy transfer processes (such as cross relaxation and/or saturation effect of intermediate levels involved in the emissions) leads to different *n* values for the two emissions. Therefore, the intensity ratio of the two upconversion emissions relies on the power density of the excitation light. In another word, the spectral shape of

upconversion emission is only meaningful when excitation condition is provided.

Theoretically, excitation density is in direct relation with initial deployment of the excited states in a nanosystem, thereby affecting the entire energy transfer process and upconversion emission properties, *e.g.* optimal doping concentration. Yet, there is no evidence suggests that the energy transfer process is excitation density dependent if excitation density is relatively low, *i.e.*<100 Wcm^{-2}. Low excitation density is usually applied to measurement of massive nanoparticles. For single nanoparticle measurement, however, high density excitation is required. Recently, Zhao *et al.* reported that, under high density excitation, upconversion emission is significantly enhanced when the concentration of activator Tm^{3+} is greatly increased.[33] As shown in Fig. 10a, the quenching concentration of Tm^{3+} ions increases with the excitation density, and reaches up to 8% under the excitation power density of 2.5×10^{6} Wcm^{-2}, much higher than 0.2~0.5% at low excitation condition (below 100 Wcm^{-2}). Similar result was also observed for Er^{3+} doped nanoparticles.[34] As shown in Fig. 10 b-e, the conventional upconversion nanoparticles (β-$NaYF_4$ with 20% Yb^{3+} and 2% Er^{3+}) is brighter than the Er^{3+}-rich upconversion nanoparticles (β-$NaYF_4$ with 20% Yb^{3+}, 25% Gd^{3+} and 20% Er^{3+}) under low excitation power density (3×10^{4} Wcm^{-2}). Increasing the excitation power density makes the Er^{3+}-rich upconversion nanoparticles brighter and brighter and finally surpass the conventional upconversion nanoparticles when the power density is above 3×10^{6} Wcm^{-2}.

The proposed physical picture is based on the initial distribution of the excited state population in the nanoparticles. Higher density excitation prepares more Yb^{3+} ions in excited state in the nanoparticles, and the critical step in upconversion emission is the excited state energy transfer from Yb^{3+} to the activator (Tm^{3+} or Er^{3+}). If the number of activators is not enough, these activators will get saturated easily in accepting excitation energy via sensitizers. From this point of view, under excitation with high density, higher doping level of activator shall promote the utilization of the excitation energy stored in the sensitizers, and facilitate the upconversion emission.

3.2.4. Surface effect

Due to the large surface-to-volume ratio of nanosystems, high proportion of lanthanide ions locates in are close to the surface. Surface properties thus become an important issue for nanotechnology. Upconversion emission was also found size-dependent.[4] Subsequently, core-shell structure was introduced to improve the upconversion emission and to study the surface effects of nanoparticles. Relevant progress has already been discussed and reviewed.[35] Here we only update our comprehension on the relevant dynamics. As mentioned in introduction, unmodified surface acts as a quenching factor for upconversion emission because it contains charged defects and/or high vibrational modes of solvents or surface-bound ligands. But the underlying quenching mechanism of upconversion emission is not yet completely clear. The interaction between the quenching centers and the activators used to be considered as "one to one" mode, *i.e.* one quenching center interacts directly with one activator without intermediates. This understanding is, however, challenged in nanomaterials. The direct interacting distance of surface effect is confirmed to be quite short (1.5~5 nm).[34,36] For a 20 nm (diameter) size nanoparticle, even take the largest surface effect distance (5 nm), there are still ~12.5% area inert to surface, which means the maximal factor of luminescence enhancement induced by shell coating should be around 8. However, this factor was reported to be more than 20 or even near two orders of magnitude when the shell thickness is only 1~2 nm.[35] These results imply that the surface quenching centers interact not only with the dopant ions within the direct interacting distance, but also with those deep inside the nanoparticle. In another word, conventional "phonon-assisted nonradiative relaxation" picture is insufficient in describing the effect of the surface related high frequency entities on the upconversion dynamics. Other processes, like energy transfer *etc.*, probably play non-negligible roles here.

Recently, there are reports that the quenching distance of the surface entities is longer than previously thought.[37] The physical picture is shown in Fig.11, the excited states of the dopants around the surface can be quenched directly by the surface quenching centers, while the energy contained in the center area of the nanoparticles might need to migrate a long distance to the surface quenching sites and be

deactivated. The efficient "long-range" energy migration was proposed to be attributed to the Gd^{3+} or Yb^{3+} medium doped in the nanoparticles.[18,28] Interestingly, this "long-range" surface quenching was found to be largely suppressed by an inert shell.

The "optimal condition" of the nanoparticle surface depends also on the application of the nanoparticles. For luminescence imaging, the strongest emission is preferred so the relatively thick shell is favored. But for FRET-relevant applications, such as photodynamic therapy shown in Fig.12, the increase of the shell thickness will, in the meantime, reduce the energy transfer efficiency from rare earth ions to the photosensitizer, therefore as a trade-off between the above two effects, an optimal thickness exists for $^1O_2$ generation.[38]

4. Enhancement of transition probability

As introduced in introduction, the transition moments responsible for the absorption and emission are subject to the local field. Therefore, they can be modified by external stimuli through variation of the local field of the sensitizers or activators. In the meantime nonradiative energy transfer processes may also be modulated by such external stimuli. For nanosystems the relevant doped ions are more susceptible to the environment due to the limited space. External stimuli induced modification of the upconversion emission properties is thus easier to be realized in nanomaterials than in macroscopic crystals.

4.1. Local crystal field adjustment

As it is confirmed, the luminescence of trivalent lanthanide ions are mostly the electric dipole transitions among the energy levels of the 4f subshell. The radiative transition is in general forbidden due to parity consideration. However, when the rare earth ions are set in an asymmetrical crystal field, the intrinsic wave functions of 4f subshell shall mix with other wave functions of opposite parity, such as the wave functions of 5d, 5g, *etc.* The transition forbidden is thus (partially) broken.[39] A high

asymmetrical crystal field is helpful in enhancing the radiative and absorption transition probabilities of rare earth ions. Some methods to change the local crystal fields in macroscopic crystals are employed also to nanosystems. For example, hexagonal $NaYF_4$:Yb^{3+},Er^{3+} nanoparticles exhibits stronger emission than their cubic counterpart. The symmetry property of the rare earth ions doped crystals can be modified in various ways. Reaction temperature is known critical to the phase formation of the crystal lattice and therefore to the consequent luminescence.[40] Adding certain ions in the crystal lattice is also helpful in reducing the crystal symmetry. For example, doping Li^+ can reduce the symmetry of the crystal field and enhance the upconversion emission.[41] Doping Gd^{3+} facilitates $NaYF_4$ host to convert from cubic phase to hexagonal.[42] These chemical methods are irreversible in nature and significant improvement in upconversion emission seems hard to reach following these approaches. In 2011, a physical approach was introduced by Hao *et al*. for nanocrystals. $BaTiO_3$ (BTO) nanohost was reported with the attractive property that the enhancement of upconversion luminescence can be realized applying external field.[43] In this work, a multi-layer film material with a typical parallel-plate capacitor was developed, in which an enhancement factor up to 2.7 was obtained for the green upconversion luminescence of Er^{3+}under a biased voltage with a maximum of 10V (limited by the breakdown voltage). According to the authors, the enhancement is attributed to the unique crystal structure of ferroelectric host material BTO. Tetragonal BTO with the point group 4mm (C_{4v}) at room temperature is non-centrosymmetric. Upon an electric field along the direction of spontaneous polarization of the host, the *c*-axis of the lattice elongates and changes the structure symmetry of the BTO host. The upconversion emission can be enhanced in a controlled manner by simply tuning the applied electric field. Difference in the enhancement of green and red emissions was analyzed based on Judd-Ofelt (*J-O*) theory. The line strength S_{ed}, which is the square of transition moment, is given by equation

$$S_{ed} = \sum_{t=2,4,6} \Omega_t |\langle 4f^n[S,L]J||U^{(t)}||4f^n[S',L']J'\rangle|^2 \qquad (3)$$

where $|4f^n[S,L]J\rangle$ and $|4f^n[S',L']J'\rangle$ are the initial and final states of the

transition, $\langle||U^{(t)}||\rangle$ is the reduced matrix elements, $\Omega_t(t = 2,4,6)$ are *J-O* intensity parameters. According to the authors, the green emission of Er^{3+} ions comes from one of the hypersensitive transitions dominated by Ω_2, which is known to be closely associated with the asymmetry of the lanthanide ion sites. This work points to another approach of enhancing upconversion emission, which could be more robust if better host materials could be explored in the future with higher breakdown voltage.

4.2. Plasma enhancement

Plasma enhancement of upconversion emission by noble metal particles is another effective approach for nanosystems. Since the discovery of noble metal surface enhanced luminescence in 1960s,[44] plasma enhancement of emission on rough noble metal surfaces has been intensively investigated for organic dyes, quantum dots and other fluorescence materials, and was recently introduced to upconversion nanomaterials.

In the past few years, nanoparticles, nanowires, nanoshells, as well as nanoarrays of Ag and Au have been employed to improve upconversion luminescence. The luminescence enhancement is in most cases attributed to the intensification of the electric field near the noble metal nanoparticle's surface by the plasma field. The intensified electric field can reinforce (i) the absorption of the upconversion nanoparticles in relation with excitation collection effect, and (ii) the emission of the activators. In addition, the nonradiative transition rates can be changed.

There are different approaches to enhance upconversion emission of nanosystems by plasmonic field. One scenario is to set the plasmonic resonance with upconversion emissions. Saboktakin *et al.* reported an enhancement of 5.2-fold by Au nanoparticles and of 45-fold by Ag nanoparticles in upconversion luminescence.[45] The enhancement, which was strongly dependent on the distance between the noble nanoparticles and the UCNPs, was attributed to the increase of both the absorption and the radiative rate of the emission. Other nanostructures of noble metals, like nanowires and nanoshells, can also improve the upconversion emission. After coupling to the noble metal, the upconversion emission lifetime was found decreased, which was argued to be the

consequence of the enhancement of radiative as well as nonradiative rates of UCNPs. Another scenario is to set the plasmonic resonance with the excitation wavelength of the upconversion emission. In 2013, plasmonic enhancement of up-conversion luminescence of nanoparticles in Au nanohole arrays was reported by Saboktakin *et al.*[46] In this study Au nanohole arrays were fabricated on transparent glass substrates. By adjusting the size of the apertures, the periodicity of the array and the thickness of the metallic layer, the plasma band of the metallic nanohole array was tuned to 980 nm - in resonance with the upconversion excitation. Based on their simulation, the electric field in the center of each aperture should be enhanced by a factor of ~6, and consequently, the absorption at 980 nm should be enhanced by a factor of ~36. The theoretical prediction was confirmed by their experiments. From optical transmission and upconversion emission spectra it was determined that the upconversion luminescence was intensified 32.6 times for the green emission around 540 nm and 34.0 times for the red emission around 650 nm. The authors thus came to the conclusion that the enhancements originated from the absorption improvement due to the resonance between the nanohole arrays and the excitation wavelength of the upconversion emission.

Plasmonic field is a powerful tool for improving the upconversion emission of nanomaterials. Very recently it was reported that the energy transfer processes are also speeded up by plasmonic field in upconversion nanomaterials.[47]

5. Conclusions and perspectives

In conclusion, we have shown that in recent years more and more attention has been drawn on the challenge of how to improve the upconversion efficiency of nanomaterials. Nanostructure brings in unique and important possibilities which their macro counterparts could not offer either in comprehension of upconversion mechanism or in application. Great efforts from various aspects, as covered in this review, have led to significant progresses in our comprehension of upconversion dynamics in nanosystems, such as the roles the surface, the “long-range migration” and the external field play in upconversion dynamics. Based on these understanding

several strategies on reduction of excitation energy loss, as well as enhancement of radiative and nonradiative transition probabilities have been proposed and executed. Despite these great efforts and achievements, in this review it is demonstrated that our comprehension of upconversion mechanism is still not sufficient for many actual applications. For example, what is the theoretical up-limit of upconversion efficiency in popular nanosystems remains a question. In detail, major excitation energy loss channels need to be thoroughly determined, and to find proper methods to avoid the channels is perhaps even more challenging. On top of that, physical pictures of the interaction between the surface related high-frequency vibrational modes and the doped rare earth ions, the role the long range energy migration plays in upconversion luminescence, the way the external fields interact with dopant ions, *et al.* need to be thoroughly elucidated.

These challenges recall scientists of different disciplines, including among others, theoretical modelling and computation, spectroscopy, synthetic chemistry and chemical engineering, to work together and an integrated effort is expected to be the solution of this formidable challenge. It is very much hoped that the answers will provide a guidance in mapping out the routes in optimizing the upconversion dynamics and will lead to the important applications in (bio-)medicine and sustainability where upconversion nanomaterials have been highly expected.

Acknowledgements

This work was supported by the Innovation Program (IOP) of the Netherland, Innovation project of the State Key Laboratory of Luminescence and Applications, Natural Science Foundation of China (No.11174277, 11374297, 61275202, 21304084, 51372096), Joint research program between KNAW of the Netherlands and CAS of China, and John van Geuns Foundation.

Figures：

Fig.1 Schematic illustration of upconversion process in rare earth ions doped nanoparticles.

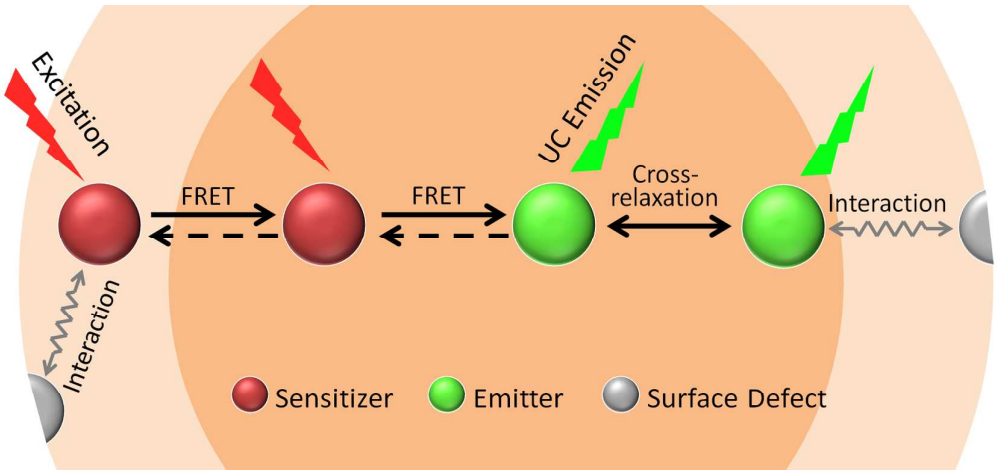

Fig.2 Schematic energy level diagrams showing typical upconversion processes for Er^{3+}. The dashed, dotted, and full arrows represent excitation, nonradiative relaxation, and emission processes, respectively.

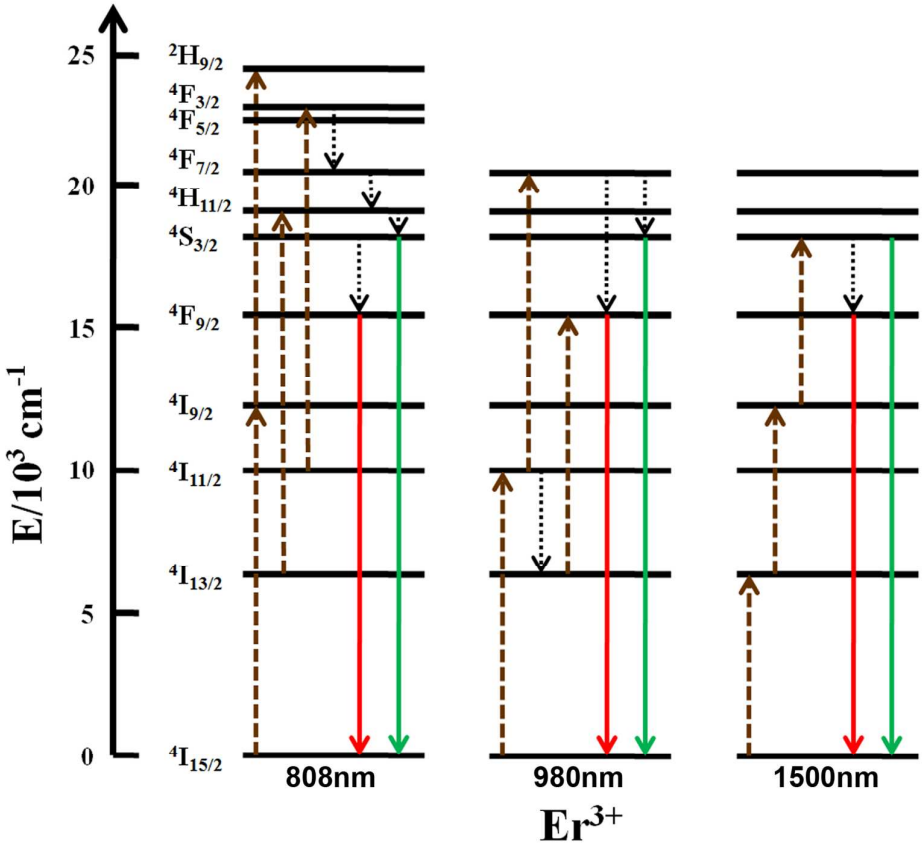

Fig. 3 Energy transfer in $NaGdF_4$: Yb^{3+}, Er^{3+}@ $NaGdF_4$: Nd^{3+}, Yb^{3+} UCNPs. (a) TEM image of $NaGdF_4$: Yb^{3+}, Er^{3+}@ $NaGdF_4$: Nd^{3+}, Yb^{3+} UCNPs and (inset) EDS line-scan profile of a single particle. (b) Energy transfer pathway from Nd^{3+}- to Yb^{3+}-activated Er^{3+} upconversion emission in core/shell structured NPs under 808 nm excitation. (c) Upconversion emission spectra of $NaGdF_4$: Yb^{3+}, Er^{3+}@ $NaGdF_4$: Nd^{3+}, Yb^{3+} UCNPs under 980 and 808 nm excitation. (Reprinted with permission from ref 10, Copyright 2013, American Chemical Society.)

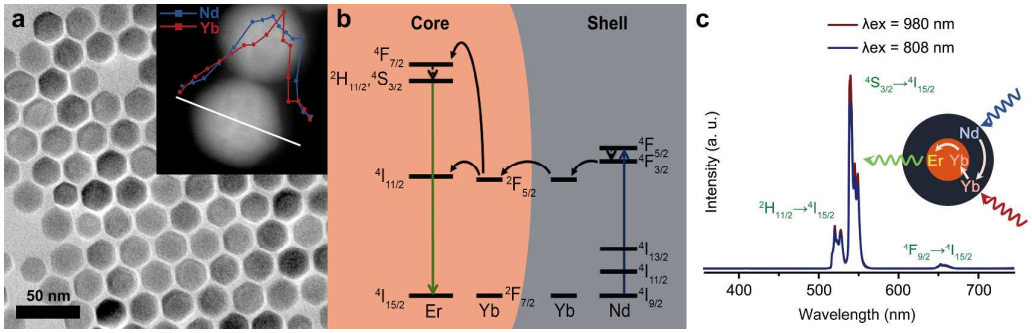

Fig. 4 Schematic illustration of basic model of ETU process.

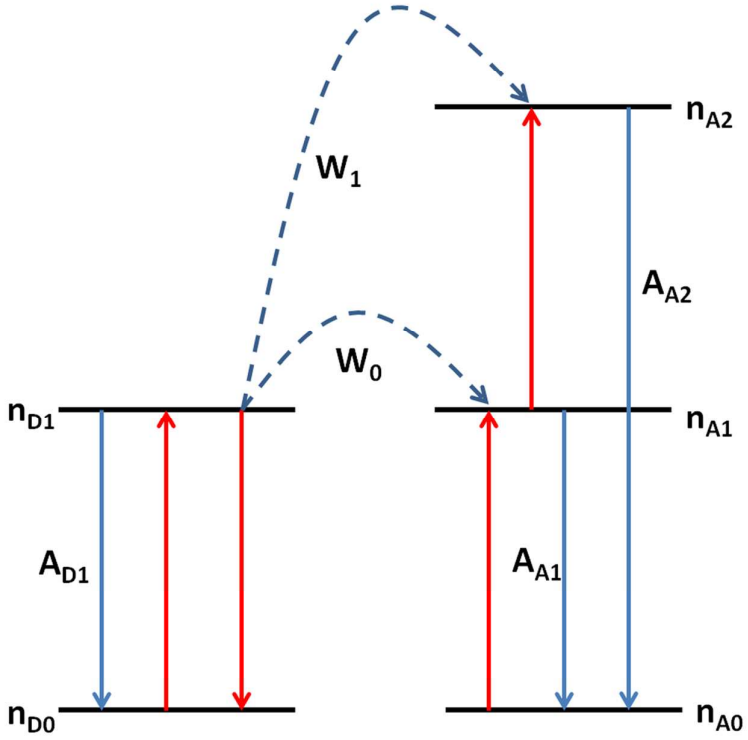

Fig.5 Energy migration-mediated upconversion (EMU) process in core-shell-shell nanoparticles. (a) Schematic design of a lanthanide-doped $NaGdF_4$ core-shell-shell nanoparticle for EMU (X: activator ion). (b) Proposed energy transfer mechanism in the core-shell-shell nanoparticle. (Reprinted with permission from ref 18, Copyright 2011, Nature publishing Group.)

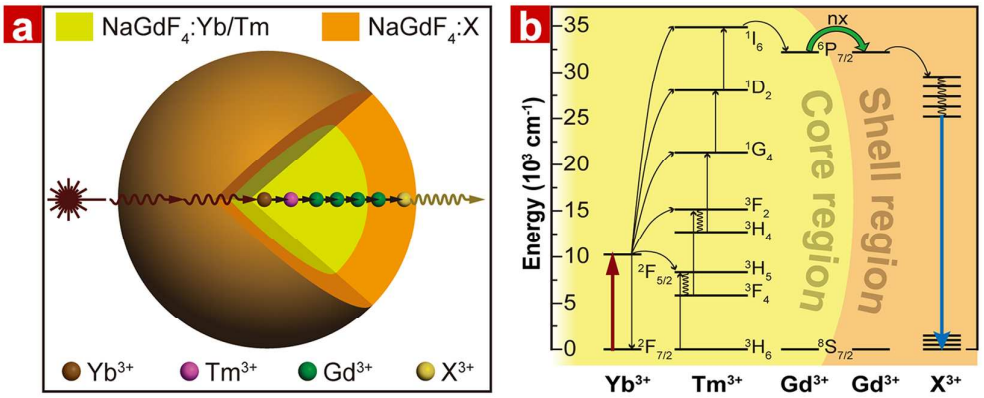

Fig. 6 (a) Schematic illustration of the core-shell-shell structure UCNPs and (b) the proposed energy-transfer mechanisms under 800 nm excitation. (Reprinted with permission from ref 13, Copyright 2013, Wiley-VCH Verlag GmbH & Co. KGaA.)

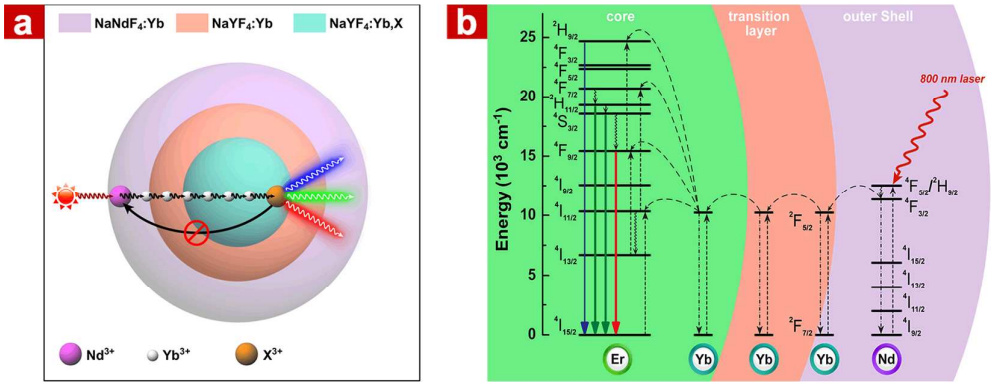

Fig. 7 Proposed energy transfer mechanisms in (a) $NaYF_4$: 2% Er^{3+}, 2% Tm^{3+} nanocrystals, and (b) Mn^{2+}-doped $NaYF_4$: Yb^{3+}/Er^{3+} (18/2 mol%) nanocrystals. (Reprinted with permission from refs. 22 and 24, Copyright 2012, American Chemical Society, Wiley-VCH Verlag GmbH & Co. KGaA.)

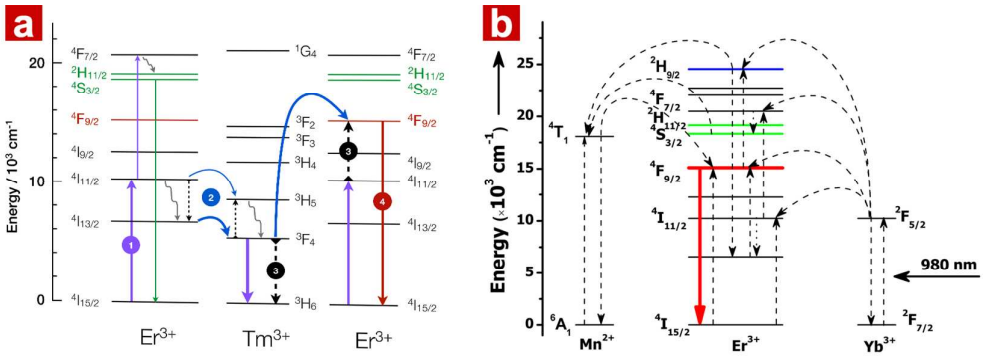

Fig. 8 (a) The classical core/active shell structure. (b) The designed emitters spatially separated structure, comprising: the core ($NaYF_4$:Yb^{3+},Er^{3+}), the first separating shell ($NaYF_4$:Yb^{3+}), the second illuminating shell (NaYF4:Yb^{3+},Er^{3+}) and the final active shell ($NaYF_4$:Yb^{3+}). (Reprinted with permission from ref 29, Copyright 2011, Royal society of Chemistry.)

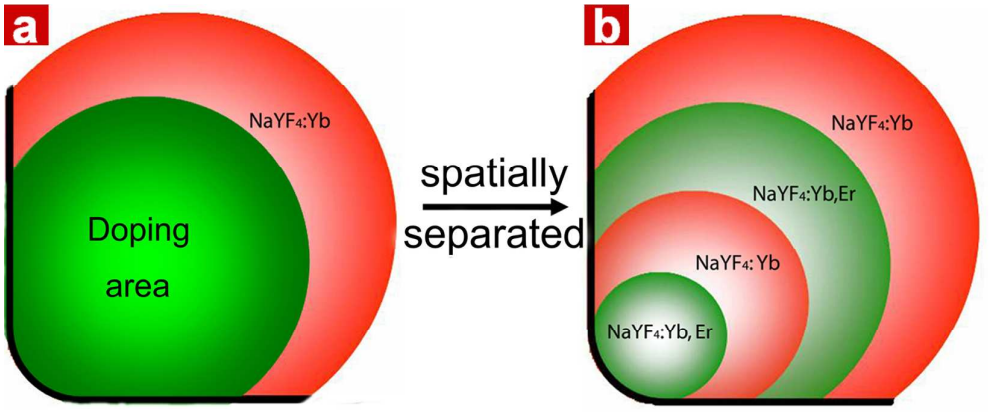

Fig. 9 Optical characterization of the KYb_2F_7: Er^{3+} nanocrystals. (a) Emission spectra of KYb_2F_7: 2% Er^{3+} (top) and KYb_2F_7: Er^{3+}, Lu^{3+} (2/0–80 mol%; bottom) nanocrystals. The inset is a typical micrograph showing the luminescence of KYb_2F_7: 2% Er^{3+} nanocrystals. (b) Proposed four-photon upconversion mechanism in KYb_2F_7: Er^{3+} nanocrystals. (c) Proposed excitation energy clustering in the Yb tetrad clusters of KYb_2F_7. (Reprinted with permission from ref 31, Copyright 2014, Nature publishing Group.)

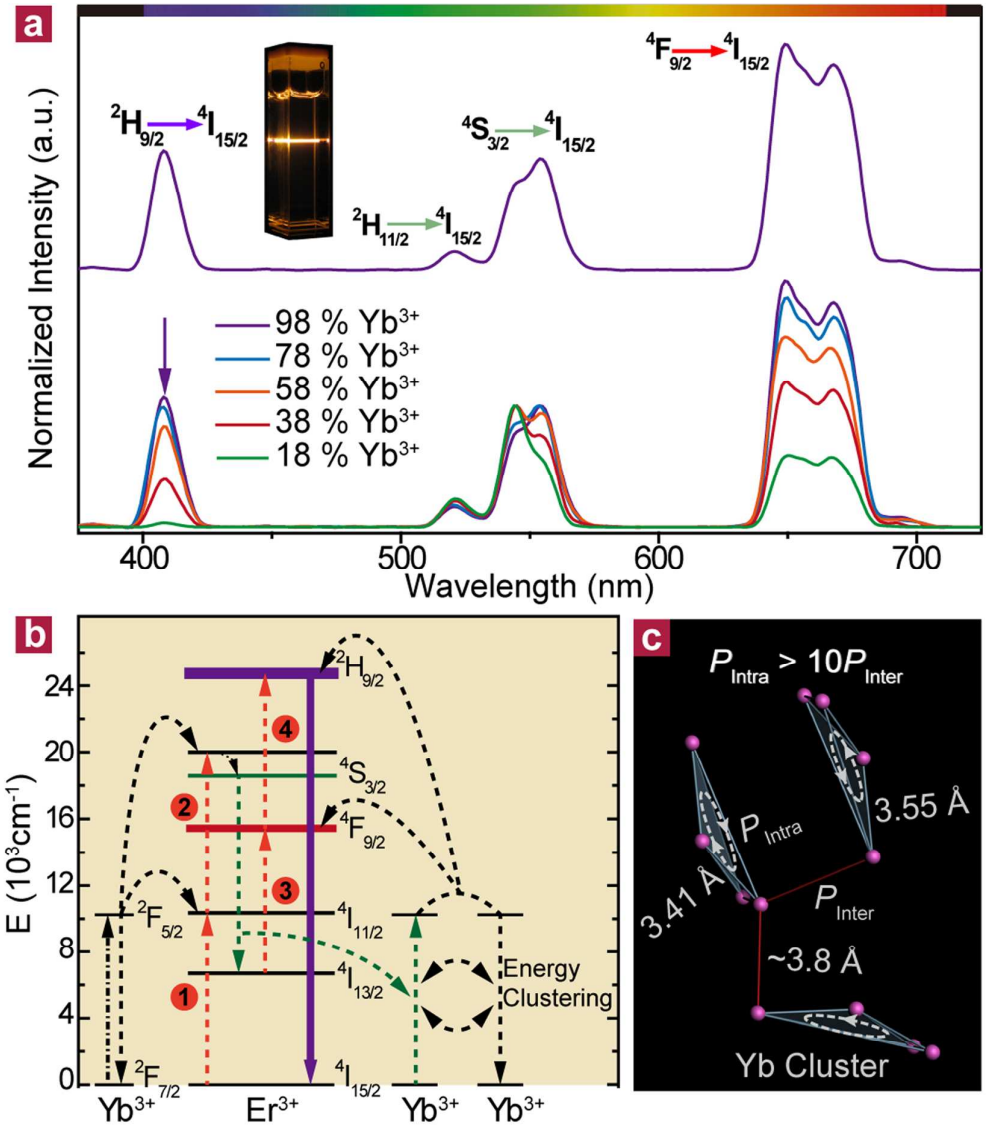

Fig. 10 (a) Integrated upconversion luminescence intensity (400 – 850 nm) *vs.* excitation density for a series of Tm^{3+} doped nanoparticles. (b) Excitation density dependent luminescence intensities of single UCNPs with 20% (blue circles) and 2% (red circles) Er^{3+}. Inset: zoom-in of the luminescence intensity cross-over region for UCNPs with the two different emitter concentrations. (c–e) Confocal luminescence images of single UCNPs containing a mixture of 2% (dashed red line) and 20% (dashed blue line) Er^{3+} under different excitation densities. Scale bar, 1mm. (Reprinted with permission from refs. 33 and 34, Copyright 2013 and 2014, Nature publishing Group.)

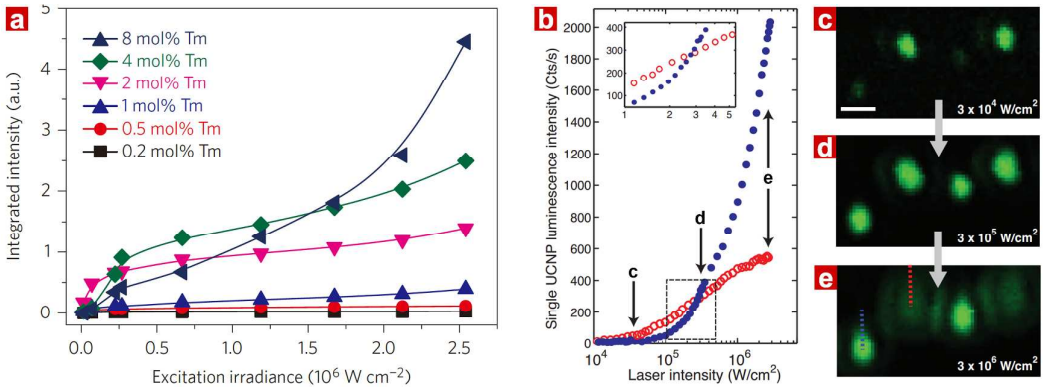

Fig. 11 Schematic illustration of the long-range surface quenching effect in the core-shell and $NaYF_4$ coated core-shell-shell nanoparticles. (Reprinted with permission from ref 37, Copyright 2012, American Chemical Society.)

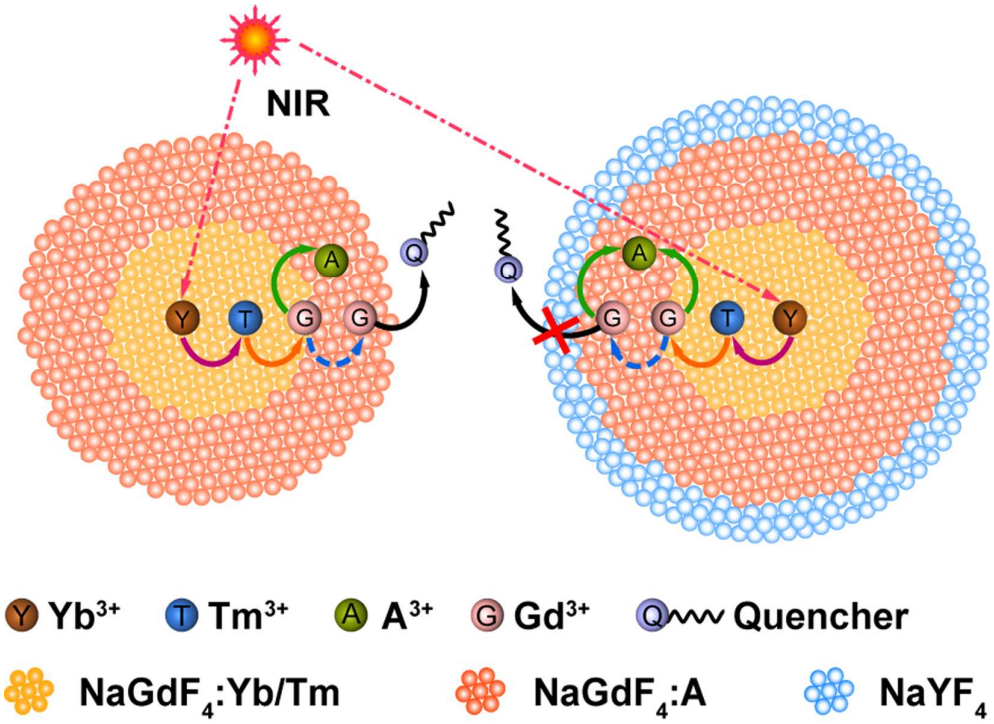

Fig. 12 Schematic illustration of the FRET process between $NaYF_4$: Yb^{3+}, Er^{3+}@$NaYF_4$ core−shell nanoparticle and photosensitizer (RB) molecule. (Reprinted with permission from ref 38, Copyright 2011, American Chemical Society.)

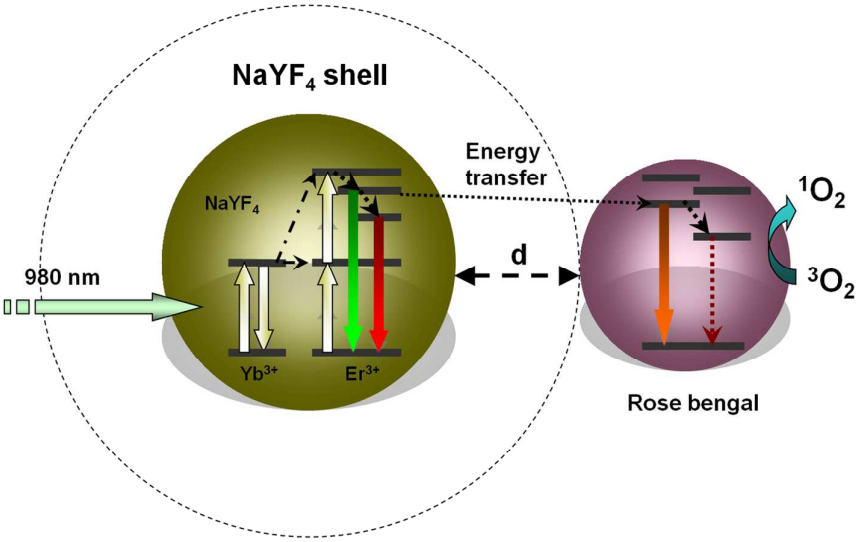

References

1. J. C. Boyer and F. van Veggel, *Nanoscale*, 2010, **2**, 1417-1419.
2. F. Auzel, *Chem. Rev.*, 2004, **104**, 139-173.
3. F. Vetrone, J. C. Boyer, J. A. Capobianco, A. Speghini and M. Bettinelli, *J. Appl. Phys.*, 2004, **96**, 661-667.
4. X. Bai, H. W. Song, G. H. Pan, Y. Q. Lei, T. Wang, X. G. Ren, S. Z. Lu, B. Dong, Q. L. Dai and L. Fan, *J. Phys. Chem. C*, 2007, **111**, 13611-13617.
5. G. Y. Chen, T. Y. Ohulchanskyy, A. Kachynski, H. Agren and P. N. Prasad, *ACS Nano*, 2011, **5**, 4981-4986.
6. R. Martin-Rodriguez, S. Fischer, A. Ivaturi, B. Froehlich, K. W. Kramer, J. C. Goldschmidt, B. S. Richards and A. Meijerink, *Chem. Mater.*, 2013, **25**, 1912-1921.
7. B. M. van der Ende, L. Aarts and A. Meijerink, *Phys. Chem. Chem. Phys.*, 2009, **11**, 11081-11095.
8. F. Vetrone, R. Naccache, V. Mahalingam, C. G. Morgan and J. A. Capobianco, *Adv. Funct. Mater.*, 2009, **19**, 2924-2929.
9. Q. Q. Zhan, J. Qian, H. J. Liang, G. Somesfalean, D. Wang, S. L. He, Z. G. Zhang and S. Andersson-Engels, *ACS Nano*, 2011, **5**, 3744-3757.
10. Y. F. Wang, G. Y. Liu, L. D. Sun, J. W. Xiao, J. C. Zhou and C. H. Yan, *ACS Nano*, 2013, **7**, 7200-7206.
11. X. F. Wang, X. H. Yan, C. X. Kan, K. L. Ma, Y. Xiao and S. G. Xiao, *Appl. Phys. B*, 2010, **101**, 623-629.
12. X. J. Xie, N. Y. Gao, R. R. Deng, Q. Sun, Q. H. Xu and X. G. Liu, *J. Am. Chem. Soc.*, 2013, **135**, 12608-12611.
13. Y. Zhong, G. Tian, Z. Gu, Y. Yang, L. Gu, Y. Zhao, Y. Ma and Y. Jiannian, *Adv. Mater.*, 2014, **26**, 2831-2837.
14. J. F. Suyver, A. Aebischer, D. Biner, P. Gerner, J. Grimm, S. Heer, K. W. Kramer, C. Reinhard and H. U. Gudel, *Opt. Mater.*, 2005, **27**, 1111-1130.
15. W. Q. Zou, C. Visser, J. A. Maduro, M. S. Pshenichnikov and J. C. Hummelen, *Nature Photon.*, 2012, **6**, 560-564.
16. M. Pollnau, D. R. Gamelin, S. R. Luthi, H. U. Gudel and M. P. Hehlen, *Phys. Rev. B*, 2000, **61**, 3337-3346.
17. W. J. C. Grant, *Phys. Rev. B*, 1971, **4**, 648-663.
18. F. Wang, R. R. Deng, J. Wang, Q. X. Wang, Y. Han, H. M. Zhu, X. Y. Chen and X. G. Liu, *Nature Mater.*, 2011, **10**, 968-973.
19. H. L. Wen, H. Zhu, X. Chen, T. F. Hung, B. L. Wang, G. Y. Zhu, S. F. Yu and F. Wang, *Angew. Chem. Int. Ed.*, 2013, **52**, 13419-13423.
20. Y. Q. Lu, J. B. Zhao, R. Zhang, Y. J. Liu, D. M. Liu, E. M. Goldys, X. S. Yang, P. Xi, A. Sunna, J. Lu, Y. Shi, R. C. Leif, Y. J. Huo, J. Shen, J. A. Piper, J. P. Robinson and D. Y. Jin, *Nature Photon.*, 2014, **8**, 32-36.
21. F. Auzel, *C. R. Acad. Sc. Paris Ser. B*, 1966, **262**, 1016.
22. G. Tian, Z. J. Gu, L. J. Zhou, W. Y. Yin, X. X. Liu, L. Yan, S. Jin, W. L. Ren, G. M. Xing, S. J. Li and Y. L. Zhao, *Adv. Mater.*, 2012, **24**, 1226-1231.

23. J. Wang, F. Wang, C. Wang, Z. Liu and X. G. Liu, *Angew. Chem. Int. Ed.*, 2011, **50**, 10369-10372.
24. E. M. Chan, G. Han, J. D. Goldberg, D. J. Gargas, A. D. Ostrowski, P. J. Schuck, B. E. Cohen and D. J. Milliron, *Nano Lett.*, 2012, **12**, 3839-3845.
25. G. Y. Chen, H. C. Liu, G. Somesfalean, H. J. Liang and Z. G. Zhang, *Nanotechnology*, 2009, **20**, 385704.
26. L. L. Wang, M. Lan, Z. Y. Liu, G. S. Qin, C. F. Wu, X. Wang, W. P. Qin, W. Huang and L. Huang, *J. Mater. Chem. C*, 2013, **1**, 2485-2490.
27. G. Y. Chen, T. Y. Ohulchanskyy, R. Kumar, H. Agren and P. N. Prasad, *ACS Nano*, 2010, **4**, 3163-3168.
28. G. Y. Chen, C. H. Yang and P. N. Prasad, *Acc. Chem. Res.*, 2013, **46**, 1474-1486.
29. X. M. Liu, X. G. Kong, Y. L. Zhang, L. P. Tu, Y. Wang, Q. H. Zeng, C. G. Li, Z. Shi and H. Zhang, *Chem. Commun.*, 2011, **47**, 11957-11959.
30. X. Teng, Y. H. Zhu, W. Wei, S. C. Wang, J. F. Huang, R. Naccache, W. B. Hu, A. I. Y. Tok, Y. Han, Q. C. Zhang, Q. L. Fan, W. Huang, J. A. Capobianco and L. Huang, *J. Am. Chem. Soc.*, 2012, **134**, 8340-8343.
31. J. Wang, R. R. Deng, M. A. MacDonald, B. L. Chen, J. K. Yuan, F. Wang, D. Z. Chi, T. S. A. Hor, P. Zhang, G. K. Liu, Y. Han and X. G. Liu, *Nature Mater.*, 2014, **13**, 157-162.
32. F. Wang and X. G. Liu, *J. Am. Chem. Soc.*, 2008, **130**, 5642-5643.
33. J. B. Zhao, D. Y. Jin, E. P. Schartner, Y. Q. Lu, Y. J. Liu, A. V. Zvyagin, L. X. Zhang, J. M. Dawes, P. Xi, J. A. Piper, E. M. Goldys and T. M. Monro, *Nature Nanotech.*, 2013, **8**, 729-734.
34. D. J. Gargas, E. M. Chan, A. D. Ostrowski, S. Aloni, M. V. P. Altoe, E. S. Barnard, B. Sanii, J. J. Urban, D. J. Milliron, B. E. Cohen and P. J. Schuck, *Nature Nanotech.*, 2014, **9**, 300-305.
35. M. Haase and H. Schafer, *Angew. Chem. Int. Ed.*, 2011, **50**, 5808-5829.
36. J. B. Zhao, Z. D. Lu, Y. D. Yin, C. McRae, J. A. Piper, J. M. Dawes, D. Y. Jin and E. M. Goldys, *Nanoscale*, 2013, **5**, 944-952.
37. Q. Q. Su, S. Y. Han, X. J. Xie, H. M. Zhu, H. Y. Chen, C. K. Chen, R. S. Liu, X. Y. Chen, F. Wang and X. G. Liu, *J. Am. Chem. Soc.*, 2012, **134**, 20849-20857.
38. Y. Wang, K. Liu, X. M. Liu, K. Dohnalova, T. Gregorkiewicz, X. G. Kong, M. C. G. Aalders, W. J. Buma and H. Zhang, *J. Phys. Chem. Lett.*, 2011, **2**, 2083-2088.
39. J. H. van Vleck, *J. Phys. Chem.*, 1937, **41**, 67-80.
40. C. H. Liu, H. Wang, X. R. Zhang and D. P. Chen, *J. Mater. Chem.*, 2009, **19**, 489-496.
41. C. Z. Zhao, X. G. Kong, X. M. Liu, L. P. Tu, F. Wu, Y. L. Zhang, K. Liu, Q. H. Zeng and H. Zhang, *Nanoscale*, 2013, **5**, 8084-8089.
42. F. Wang, Y. Han, C. S. Lim, Y. H. Lu, J. Wang, J. Xu, H. Y. Chen, C. Zhang, M. H. Hong and X. G. Liu, *Nature*, 2010, **463**, 1061-1065.
43. J. H. Hao, Y. Zhang and X. H. Wei, *Angew. Chem. Int. Ed.*, 2011, **50**, 6876-6880.
44. K. H. Drexhage, *Bull. Am. Phys. Soc.*, 1969, **14**, 873.
45. M. Saboktakin, X. C. Ye, S. J. Oh, S. H. Hong, A. T. Fafarman, U. K. Chettiar, N. Engheta, C. B. Murray and C. R. Kagan, *ACS Nano*, 2012, **6**, 8758-8766.
46. M. Saboktakin, X. C. Ye, U. K. Chettiar, N. Engheta, C. B. Murray and C. R. Kagan, *ACS Nano*, 2013, **7**, 7186-7192.
47. Q. C. Sun, H. Mundoor, J. C. Ribot, V. Singh, Smalyukh, II and P. Nagpal, *Nano Lett.*, 2014, **14**, 101-106.